Cell Insight 2 (2023) 100088

Contents lists available at ScienceDirect

Cell Insight

journal homepage: www.journals.elsevier.com/cell-insight

Research Article

Inhibition of TRPP3 by calmodulin through Ca^{2+}/calmodulin-dependent protein kinase II

Xiong Liu [a], Yifang Wang [a,b], Ziyi Weng [a,b], Qinyi Xu [a], Cefan Zhou [b], JingFeng Tang [b,**], Xing-Zhen Chen [a,b,*]

[a] Membrane Protein Disease Research Group, Department of Physiology, Faculty of Medicine and Dentistry, University of Alberta, T6G 2H7, Edmonton, AB, Canada
[b] National "111" Center for Cellular Regulation and Molecular Pharmaceutics, Hubei University of Technology, Wuhan, Hubei, 430068, China

HIGHLIGHTS

- CaM inhibits the function of TRPP3.
- CaM N-lobe interacts with TRPP3 C-terminal fragment I560–F621 and this interaction is Ca^{2+} dependent.
- CaM inhibits the function of TRPP3 through promoting CaMK2's phosphorylation towards T591 on TRPP3.

GRAPHICAL ABSTRACT

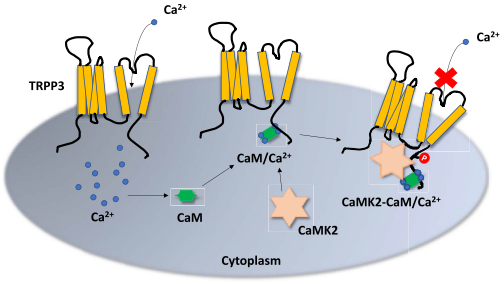

ARTICLE INFO

Keywords:
TRP channel
CaM
Calcium
CaMK2
Electrophysiology
Xenopus oocyte

ABSTRACT

Transient receptor potential (TRP) polycystin-3 (TRPP3) is a non-selective cation channel activated by Ca^{2+} and protons and is involved in regulating ciliary Ca^{2+} concentration, hedgehog signaling and sour tasting. The TRPP3 channel function and regulation are still not well understood. Here we investigated regulation of TRPP3 by calmodulin (CaM) by means of electrophysiology and *Xenopus* oocytes as an expression model. We found that TRPP3 channel function is enhanced by calmidazolium, a CaM antagonist, and inhibited by CaM through binding of the CaM N-lobe to a TRPP3 C-terminal domain not overlapped with the EF-hand. We further revealed that the TRPP3/CaM interaction promotes phosphorylation of TRPP3 at threonine 591 by Ca^{2+}/CaM-dependent protein kinase II, which mediates the inhibition of TRPP3 by CaM.

1. Introduction

The mammalian transient receptor potential (TRP) superfamily of ion channels comprises six subfamilies: TRPC (canonical), TRPM (melastatin), TRPML (mucolipin), TRPP (polycystin), TRPV (vanilloid) and TRPA (ankyrin). TRP channels respond to a variety of stimuli, ranging from temperature, natural chemicals, pH, to mechanical force (Vangeel & Voets, 2019). TRPP3, also called polycystic kidney disease (PKD) protein 2 like 1 (PKD2L1), was first identified in 1998 (Nomura et al., 1998). Although mutations in its homologue protein TRPP2 (or PKD2) and

* Corresponding author. Membrane Protein Disease Research Group, Department of Physiology, Faculty of Medicine and Dentistry, University of Alberta, T6G 2H7, Edmonton, AB, Canada.
** Corresponding author. National "111" Center for Cellular Regulation and Molecular Pharmaceutics, Hubei University of Technology, Wuhan, Hubei, 430068, China.
E-mail addresses: tangjingfeng@hbut.edu.cn (J. Tang), xzchen@ualberta.ca (X.-Z. Chen).

https://doi.org/10.1016/j.cellin.2023.100088
Received 14 December 2022; Received in revised form 2 February 2023; Accepted 3 February 2023
Available online 9 February 2023

membrane receptor PKD protein 1 (PKD1) account for 15% and 80%, respectively, of human autosomal dominant PKD (ADPKD) (Pei, 2003), TRPP3 is unlikely involved in the disease. Despite of its wide tissue distribution, including heart, skeletal muscle, brain, spleen, testis, retina and liver (Nomura et al., 1998; Wu et al., 1998), its physiological roles have not been well documented. TRPP3 forms a heterotetrameric channel with PKD protein 1 like 1 (PKD1L1) and 3 (PKD1L3) (DeCaen et al., 2013; Ishimaru et al., 2006). The TRPP3/PKD1L1 complexing was reported to control Ca^{2+} concentration in primary cilia through a Ca^{2+}-dependent hedgehog signaling pathway, which seems to be developmentally important (DeCaen et al., 2013; Delling et al., 2013). TRPP3 regulates body fluid homeostasis and heart function during pathological cardiac hypertrophy (Lu et al., 2018). TRPP3 in cerebrospinal fluid-contacting neurons is important for the maintenance of natural curvature of the spine in zebrafish (Sternberg et al., 2018).

CaM is a ubiquitous Ca^{2+}-binding protein with four EF-hand motifs forming two globular lobes (N- and C-lobes). Ca^{2+} binds to each lobe and triggers a structural rearrangement that changes the affinity of CaM binding to other target proteins such as voltage-gated Na^+, K^+ channels (Gabelli et al., 2016; Wen & Levitan, 2002), cyclic nucleotide-gated channels (Trudeau & Zagotta, 2002), and TRP channels (Mercado et al., 2010). A growing body of reports have demonstrated the involvement of CaM in the functional regulation of several TRP channels (Hasan & Zhang, 2018), possibly through a shared mechanism. CaM antagonist calmidazolium (CMZ) was reported to activate TRPP3 but with an unclear mechanism (DeCaen et al., 2013; Park et al., 2018).

In the present study, we examined how CaM regulates TRPP3 channel function by the two-electrode voltage clamp (TEVC) electrophysiology in *Xenopus* oocytes. We characterized the interaction between CaM and TRPP3 by means of co-immunoprecipitation (co-IP) and *in vitro* Pull-down and examined the interplay among CaM, membrane-anchored phosphatidylinositol 4,5-bisphosphate (PIP2) and Ca^{2+}/CaM-dependent protein kinase II (CaMK2) with respect to the regulation of TRPP3.

2. Results

2.1. CMZ activates TRPP3 in Xenopus oocytes

By means of the TEVC electrophysiology in *Xenopus* oocytes we verified that the channel activity of TRPP3 is enhanced by CMZ, an inhibitor of CaM (Fig. 1 A and B). The TRPP3 channel activity at −50 mV was assessed by the current elicited by 5 mM Ca^{2+} in the Na^+-containing bath solution that included 10 μM 2-[(4-methoxynaphthalen-2-yl) amino]-5-nitrobenzoic acid (MONNA) to inhibit currents mediated by endogenous Cl channels activated by Ca^{2+} entry, similarly as we did previously (Cai et al., 2020; Wang et al., 2019). The stimulation effect of CMZ was also observed in other membrane potentials using a voltage ramp protocol (Fig. 1C). Of note, the basal TRPP3 channel activity, assessed by the difference of current between Na^+-containing solution and one that contains non-permeant NMDG, both in the absence of Ca^{2+}, was also enhanced by CMZ to a similar extent (Fig. 1 D, E and F). This CMZ-induced stimulation of the basal TRPP3 function is comparable to what was reported for TRPP3 expressed in human embryonic kidney (HEK) cells (DeCaen et al., 2013; Park et al., 2018). Our data suggested possible involvement of CaM as a TRPP3 inhibitor.

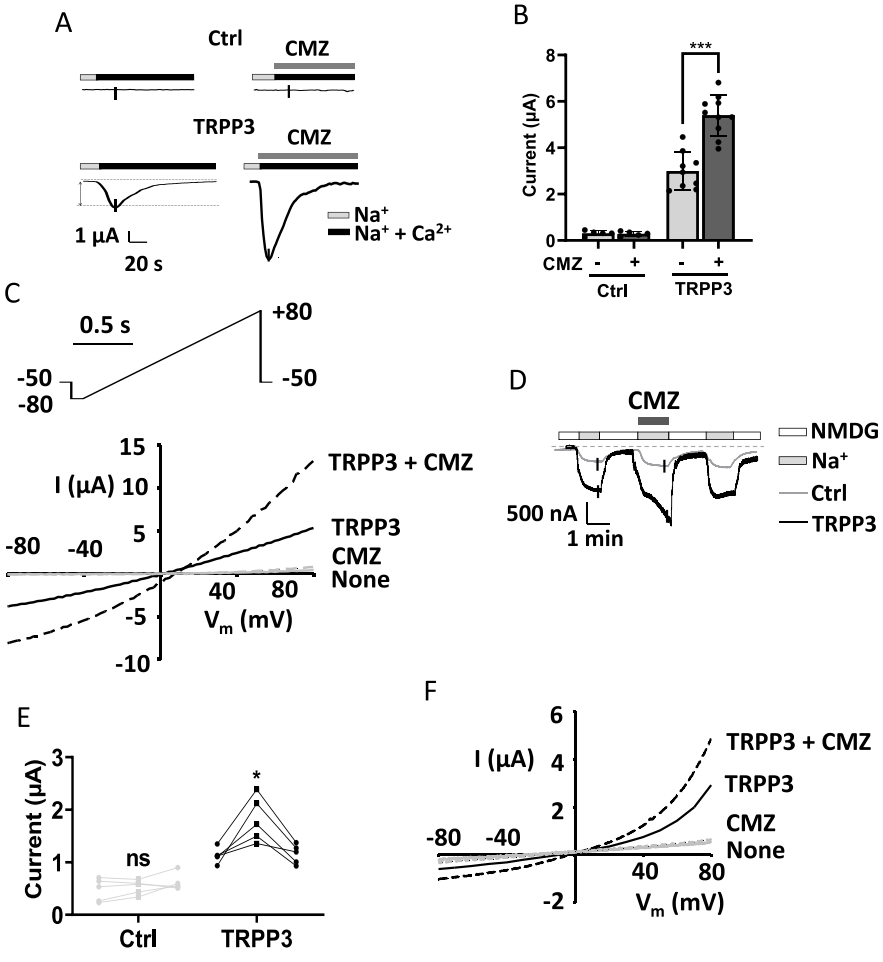

Fig. 1. Effect of CMZ on TRPP3 channel function. **A.** Representative whole-cell current traces obtained from a water-injected oocyte (Ctrl) and one expressing human TRPP3. Oocytes were clamped at −50 mV and perfused with the Na^+-containing solution ("Na^+") (in mM) (100 NaCl, 2 KCl, 1 $MgCl_2$, 10 HEPES, pH 7.5), or one added with 5 mM $CaCl_2$ ("Na^+ + Ca^{2+}"), in the presence of 10 μM MONNA throughout. TRPP3 channel activity was measured as the Ca^{2+}-induced peak current ("Na^+ + Ca^{2+}") (i.e., current at "Na^+ + Ca^{2+}" minus current at "Na^+"). 10 μM CMZ was applied, as indicated. **B.** Averaged Ca^{2+}-induced currents obtained from Ctrl oocytes and those expressing TRPP3, under the same experimental conditions as in panel A. ***$p < 0.001$. **C.** Representative I–V curves obtained from a Ctrl and TRPP3-expressing oocyte, using a ramp protocol (with voltages, in mV, as indicated) applied at time points indicated by vertical bars in panel A traces. **D.** Representative whole-cell current traces recorded by TEVC at −50 mV from a Ctrl and TRPP3-expressing oocyte. Oocytes were perfused with Na^+-containing solution or one with equimolar N-methyl-D-glucamine (NMDG) replacing Na^+ (NMDG). 10 μM CMZ was applied, as indicated. **E.** Averaged Na currents from Ctrl and TRPP3-expressing oocytes. *$p < 0.05$. Na^+ currents were determined as the difference between the plateau ("Na^+") and baseline ("NMDG") values. **F.** Representative I–V curves from a Ctrl and TRPP3-expressing oocyte, using the ramp protocol (as in panel C) applied at time points indicated by vertical bars in panel E traces.

2.2. The TRPP3/CaM physical association

We first tested whether CaM indeed regulates the TRPP3 channel function. By co-expressing TRPP3 and CaM in oocytes, we found that CaM substantially decreases both the basal and Ca^{2+}-activated currents (Fig. 2A). To figure out whether CaM inhibited the TRPP3 channel function or decreased the TRPP3 surface membrane expression we performed biotinylation assays and found that CaM does not have significant effect on the surface expression (Fig. 2B), indicating that CaM inhibits TRPP3. These data also indicated that CMZ increases the TRPP3 channel activity through inhibiting CaM. Given that CaM interacts with different channels to regulate the channel function, we next wanted to investigate whether CaM physically interacts with TRPP3. For this, we performed co-IP assays using Flag-TRPP3 and HA-CaM for expression in oocytes and found that they are indeed in the same complex (Fig. 2C). We also carried out *in vitro* Pull-down assays using CaM-coated agarose beads to incubate with lysates of TRPP3-expressing oocytes at different concentrations of Ca^{2+}. We found that the TRPP3/CaM interaction is Ca^{2+}-dependent (Fig. 2D). Besides, the TRPP3/CaM interaction was inhibited by CMZ (Fig. 2E), further supporting that CMZ activates TRPP3 through antagonizing CaM.

2.3. The TRPP3/CaM binding is mediated by the CaM N-lobe and TRPP3 C-terminal fragment I560–F621

As a versatile Ca^{2+} sensor, CaM is capable of regulating various processes through Ca^{2+} binding at its two different lobes (Chin & Means, 2000). To further elucidate the functional significance of the Ca^{2+}-dependent TRPP3/CaM interaction we altered Ca^{2+} binding in CaM mutants CaM_{12} (with double mutation D20A/D56A), CaM_{34} (D93A/D129A) and CaM_{1234} (quadruple mutation D20A/D56A/-D93A/D129A), representing D-to-A mutations within the Ca^{2+}-binding sites in the N-lobe, C-lobe and both lobes, respectively. We found that each of CaM and CaM_{34}, but not CaM_{12} or CaM_{1234}, are able to inhibit the TRPP3 channel function (Fig. 3A), while none of these mutants altered the plasma expression of TRPP3 (Fig. 3B). These data indicated that Ca^{2+} binding to the CaM N-lobe, but not the C-lobe, is critical for its regulation of TRPP3 and supported the concept that the two lobes can work independently (Stefan et al., 2008). We further found that the N-lobe, but not the C-lobe, is important for the TRPP3/CaM binding. (Fig. 3C). Taken together, the data indicated that the N-lobe of CaM mediates its binding with and functional regulation of TRPP3.

We next wanted to identify the CaM-binding domain (CaMBD) in TRPP3. CaMBDs in several TRP channels are located in the N- or C-terminus and predicted to be mostly hydrophobic alpha helices (Gordon--Shaag et al., 2008). It was predicted that CaM-binding site in TRPP3 is located in the C-terminus (Park et al., 2019), but so far there have been no supporting experimental data. We therefore generated TRPP3 truncation mutants with deletion of the N-terminus (named P3ΔN) or C-terminus (P3ΔC) and tested their interaction with CaM by Pull-down assays using CaM-coated agarose beads. We found that mutant P3ΔN but not P3ΔC exhibits similar strength of binding with CaM as WT TRPP3 (Fig. 3D), indicating that TRPP3 indeed contains a CaM-binding site in the C-terminus. We also performed *in vitro* Pull-down experiments to further document the TRPP3/CaM interaction. For this, we constructed glutathione S-transferase (GST)-tagged CaM and His-tagged C-terminal peptide I560–K660 (called His-P3CP) and purified from *E. coli* expression. By using GST and GST-tagged TRPP3 N-terminal peptide M1-L95 (GST-P3NP) as negative and positive controls, respectively (Zheng et al., 2018), we confirmed that His-P3CP directly binds with GST-CaM (Fig. 3E). We next wanted to examine whether the EF-hand motif (H633-E668) within TRPP3 C-terminus plays a role in the interaction with CaM. The EF-hand motif in the C-terminus of other channels was reported to mediate binding with CaM (Ben Johny et al., 2013). We found by co-IP and Pull-down experiments that, compared with WT TRPP3, truncation mutant T622X that lacks the majority of the

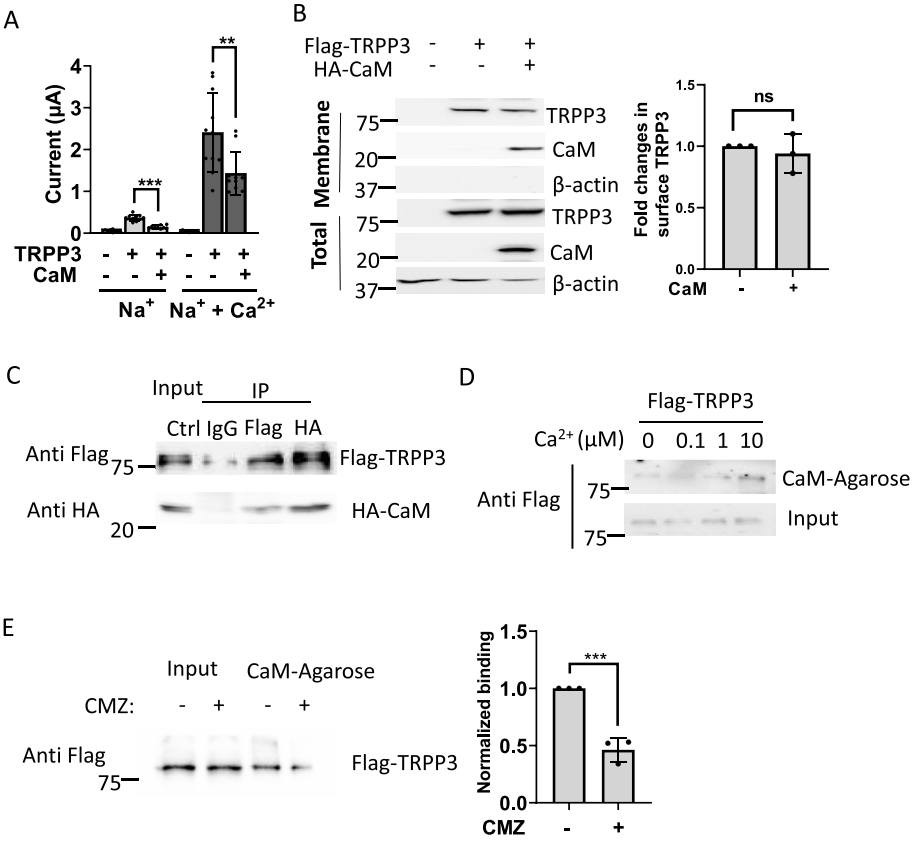

Fig. 2. Effect of CaM on TRPP3 channel function and physical interaction between TRPP3 and CaM. **A.** Averaged basal ("Na^+") current and Ca^{2+}-activated current (= current at "$Na^+ + Ca^{2+}$" minus current at "Na^+") measured in Ctrl and TRPP3-expressing oocytes, with or without CaM, using TEVC from three independent experiments. Correspondingly, the Na^+-containing solution with 5 mM $CaCl_2$ ("$Na^+ + Ca^{2+}$") or without Ca^{2+} ("Na^+") was used. $^{**}p < 0.01$; $^{***}p < 0.001$; by One-way ANOVA with Holm-Sidak's correction. **B.** Left panel: representative surface and total expression of TRPP3 and CaM determined by biotinylation, with β-actin as a loading control. Right panel: data from three independent experiments were quantified, normalized, and averaged. ns: not significant. **C.** Representative co-IP data of three independent experiments, showing interaction between TRPP3 and CaM. **D.** Representative CaM-Agarose Pull-down data of three independent experiments, showing direct TRPP3/CaM binding as a function of the Ca^{2+} concentration. **E.** Left panel: representative CaM-Agarose Pull-down data, showing the effect of CMZ on the direct TRPP3/CaM binding. Right panel: data from three independent experiments were quantified, normalized, and averaged. $^{***}p < 0.001$.

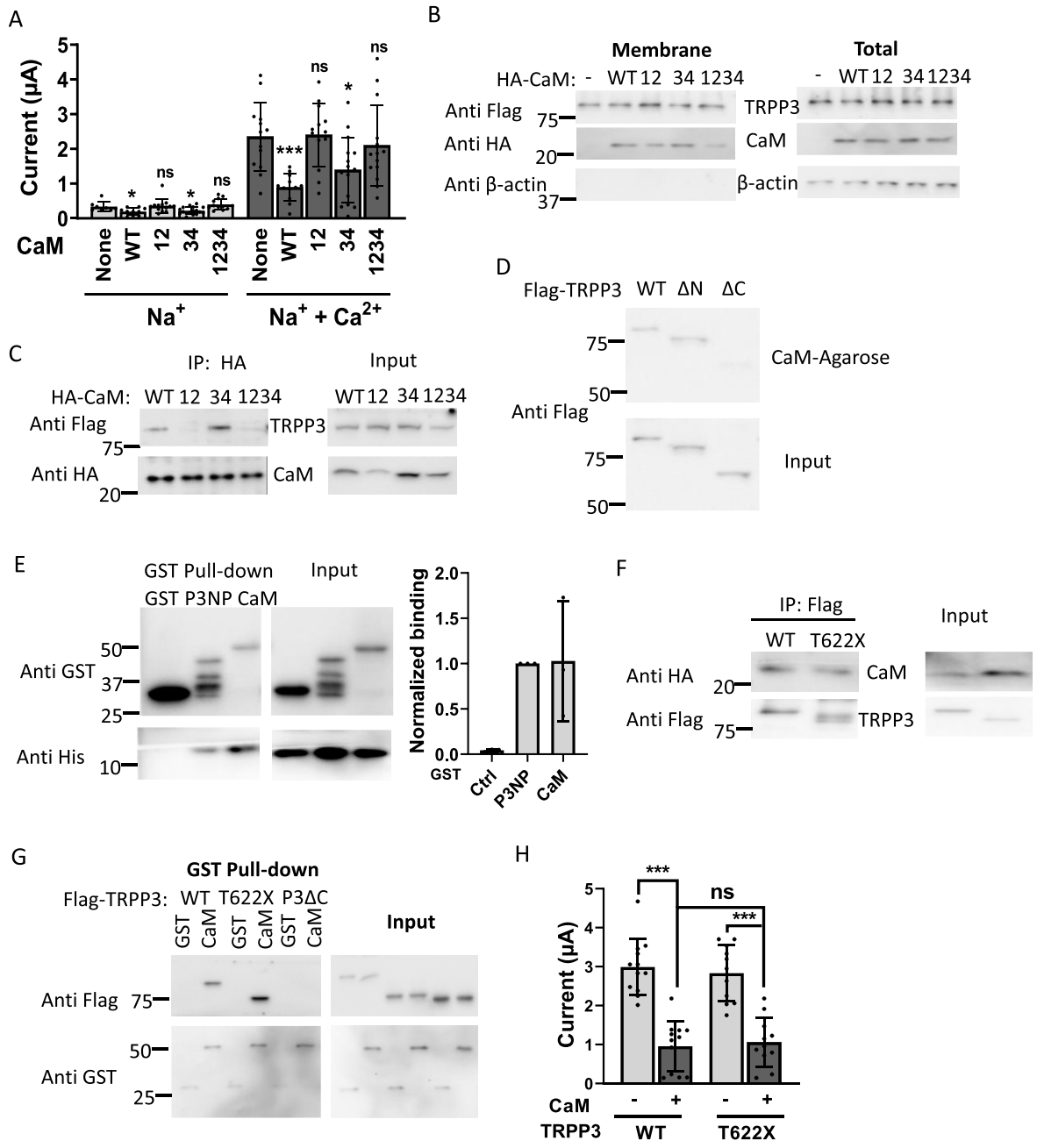

Fig. 3. Domains of interaction between CaM and TRPP3. A-C. Flag-TRPP3 was expressed in oocytes alone or with HA-tagged WT or a mutant CaM (CaM_{12}, CaM_{34} or CaM_{1234}). **A.** Averaged basal ("Na^+") and Ca^{2+}-activated ("$Na^+ + Ca^{2+}$" minus "Na^+") currents from three independent experiments measured using TEVC in the presence of the Na-containing solution with ("$Na^+ + Ca^{2+}$") or without ("Na^+") 5 mM $CaCl_2$. *$p < 0.05$; ns: not significant. **B.** Surface and total expression of TRPP3 and CaM mutants determined by biotinylation as representative data of three independent experiments, with β-actin as a loading control. **C.** Representative co-IP data of three independent experiments, showing the interaction between TRPP3 and a CaM mutant. **D.** Representative CaM-Agarose Pull-down data of three independent experiments, showing direct interaction of CaM with WT TRPP3, P3ΔN or P3ΔC. **E.** Left panel: representative GST Pull-down data showing direct interaction of His-P3CP with GST-tagged CaM with purified GST and GST-P3NP as negative and positive controls, respectively. Right panel: data from three independent experiments, as in left panel, were quantified, normalized, and averaged. **F.** Representative co-IP data of three independent experiments, showing the interaction of HA-CaM with Flag-TRPP3 (WT or mutant T622X). **G.** Representative GST Pull-down data of three independent experiments, showing the interaction of GST-CaM (with GST as control) with Flag-tagged TRPP3 WT, truncation mutant T622X, or P3ΔC (Ctrl). **H.** Ca^{2+}-activated currents of WT TRPP3 or mutant T622X with or without CaM co-expression in oocytes were averaged from three independent experiments in the Na^+-containing solution. ***$p < 0.001$; ns: not significant.

C-terminus including the EF-hand motif has similar CaM-binding strength (Fig. 3 F and G). Further, CaM had a similar inhibitory effect on the WT TRPP3 and mutant T622X (Fig. 3H), indicating that EF-hand is unlikely involved in CaM regulation. Taken together, these data indicated that the TRPP3 C-terminal fragment I560–F621 is a CaM-binding domain.

2.4. CaM and PIP2 competitively bind with TRPP3 but with distinct mechanisms of inhibition

We recently reported that PIP2 interacts with the TRPP3 C-terminal domain 594-RLRLRK-599, which disrupts the functionally critical intramolecular interaction between the N- and C-terminus of TRPP3 (called

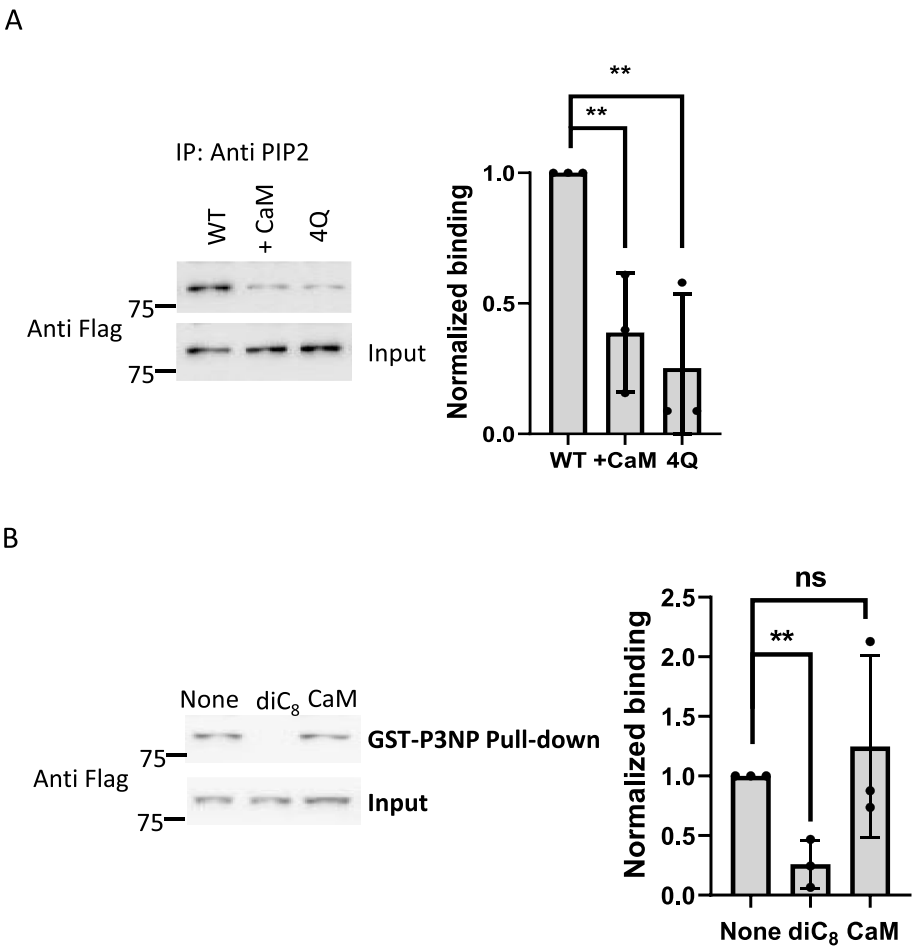

Fig. 4. Relationship of CaM and PIP2 on TRPP3 regulation. A. Left panel: representative co-IP data showing the effect of CaM on the interaction of diC8 PIP2 (a water-soluble dioctanoyl analog of PIP2) with TRPP3, with TRPP3 4Q mutant (R594Q/R596Q/R598Q/K599Q quadruple mutant) as a control. Right panel: data from three independent experiments in left panel were quantified, normalized, and averaged. $^{**}p < 0.01$. **B.** Left panel: representative GST Pull-down data showing the effect of CaM on the interaction between GST-P3NP and Flag-TRPP3 FL, with diC8 PIP2 as a positive control. Right panel: data from three independent experiments, as in left panel, were quantified, normalized, and averaged. $^{**}p < 0.01$; ns: not significant.

the N/C binding), thereby inhibiting the channel function (Zheng et al., 2018). Because 594-RLRLRK-599 is within the CaM-binding domain I560–F621, it is possible that PIP2 and CaM interfere with each other with respect to their binding to TRPP3 so that both exhibit an inhibitory effect on the channel function. We found that CaM indeed significantly reduces the TRPP3/PIP2 binding (Fig. 4A), in support of the possibility that CaM and PIP2 compete with each other for physical binding with TRPP3. We next wondered whether CaM, like PIP2 (Zheng et al., 2018), inhibits TRPP3 through disrupting the N/C interaction. For this, we assessed the TRPP3 N/C binding using purified GST-P3NP and over-expressed full-length TRPP3 by GST Pull-down assays. Interestingly, unlike PIP2, CaM had no significant effect on the N/C binding (Fig. 4B). Taken together, our data indicated that CaM and PIP2 inhibit the TRPP3 channel function through distinct mechanisms even though they compete with each other for binding with TRPP3.

2.5. *CaMK2 mediates the regulation of TRPP3 by CaM*

We next wanted to examine how CaM suppresses the TRPP3 channel function. Because phosphorylated TRPP3 exhibits greatly reduced function (Zheng et al., 2016), we wondered whether CaM-dependent downstream kinase CaMK2 is involved in the phosphorylation of TRPP3. We first found that treatment with KN93 or myristoylated autocamtide-2 related inhibitory peptide (AIP), potent inhibitors of CaMK2, significantly increases the TRPP3 channel activity (Fig. 5A). We next co-expressed TRPP3 with CaMK2 dominant negative mutant K42M or constitutively active mutant T286D (Sun et al., 2008) and found that the CaMK2 kinase activity is inversely correlated with the TRPP3 channel activity, with the TRPP3 surface membrane expression unaltered by CaMK2 co-expression (Fig. 5 B and C). Further, by co-IP experiments we found that CaMK2 and TRPP3 are in the same complex (Fig. 5D). These data together strongly suggested that phosphorylation of TRPP3 by CaMK2 may underlie the inhibition of TRPP3 by CaM. We also found that expression of CaM, but not that of Ca2+-insensitive mutant CaM_{1234}, significantly enhances the TRPP3/CaMK2 interaction (Fig. 5E). Taken together, our data suggest that Ca^{2+}/CaM binding with TRPP3 may recruit CaMK2 to TRPP3 to facilitate phosphorylation and thereby functional inhibition of TRPP3.

We next wanted to determine whether and how CaMK2 phosphorylates TRPP3. CaMK2 has a general phosphorylation motif RXX[S/T] in its target proteins (Songyang et al., 1996) but several exceptions have been reported (Dosemeci & Jaffe, 2010; Huang et al., 2011; White et al., 1998). Because there is no such a motif in and near the TRPP3 CaMBD, based on enhanced TRPP3/CaMK2 interaction by CaM, we decided to test three candidate phosphorylation sites S581, T591 and S603 within CaMBD through alanine and glutamate substitutions to mimic dephosphorylation and phosphorylation, respectively (Fig. 6A). We found mutations T591A and T591E substantially increases and decreases the channel function, respectively, while none of the mutations at S581 and S603 affected the function (Fig. 6 B and C). Consistently, mutant T591A was no longer inhibitable by constitutively active mutant CaMK2-T286D (Fig. 6D), strongly indicating that T591 phosphorylation by CaMK2 is involved in TRPP3 inhibition.

Because CaM binds with TRPP3 independently of CaMK2, we wondered whether CaM inhibits TRPP3 function also (in part) through the TRPP3/CaM binding. By CaM agarose beads Pull-down experiments, we found that the two mutations at T591 do not affect the TRPP3/CaM binding (Fig. 6E) but that mutation T591A abolishes the inhibitory effect

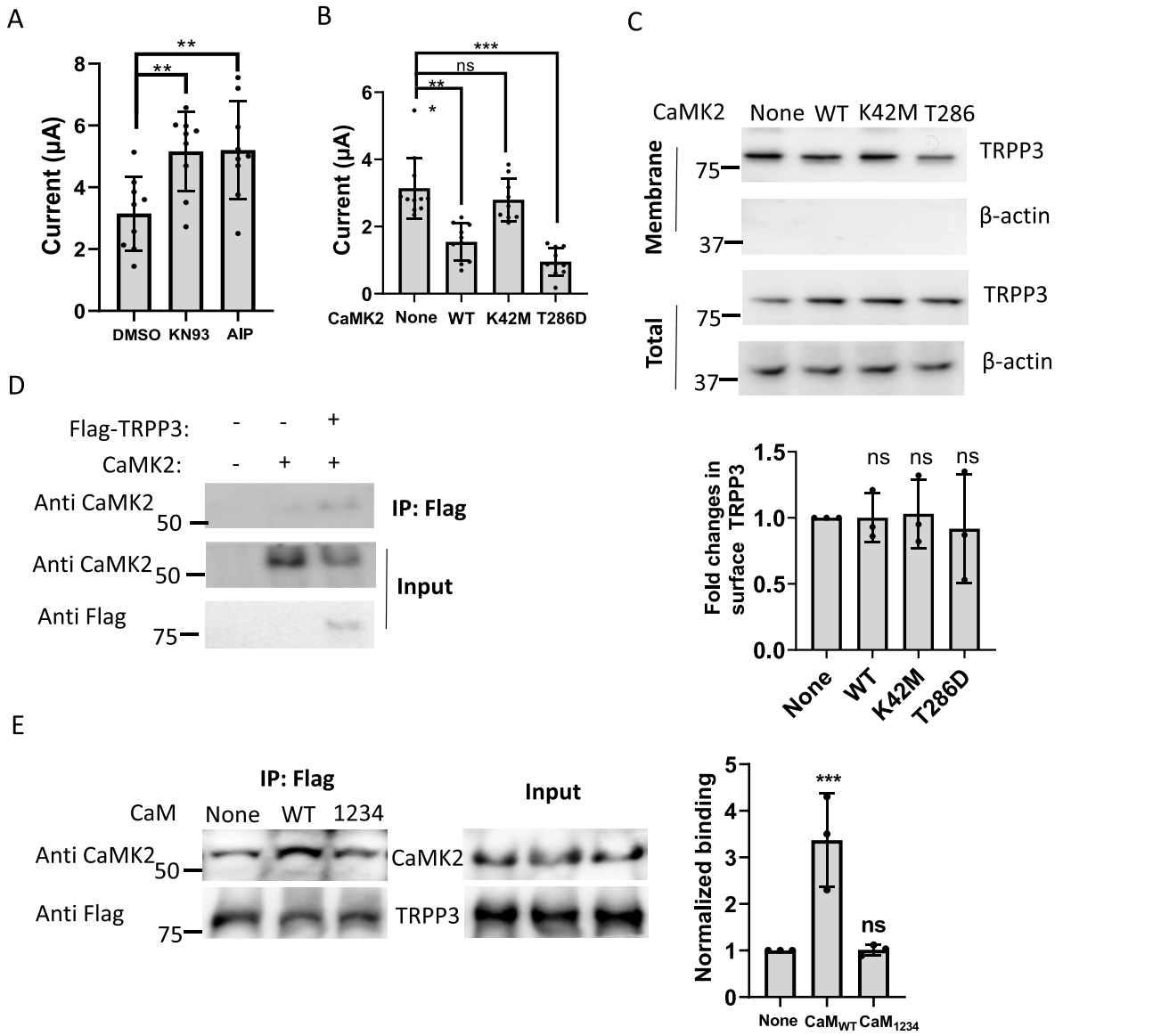

Fig. 5. Effect of CaMK2 on TRPP3 channel function. A. Ca^{2+}-activated currents (at −50 mV) averaged from three batches of TRPP3-expressing oocytes after treatment with 10 μM KN93, 10 μM AIP or 0.1% DMSO (Ctrl) for 30 min $^{**}p < 0.01$. **B.** Averaged Ca^{2+}-activated currents (at −50 mV) obtained from three batches of oocytes co-expressing TRPP3 with an indicated CaMK2 mutant or none. $^{***}p < 0.001$; ns: not significant. **C.** Effects of CaMK2 mutants on the TRPP3 expression on the oocyte surface. Upper panel: representative surface and total expression of TRPP3 determined by biotinylation, with β-actin as a loading control. Lower panel: data from three independent experiments were quantified, normalized, and averaged. ns: not significant. **D.** Representative co-IP data of three independent experiments, showing the interaction between TRPP3 and CaMK2. **E.** Left panel: representative co-IP data showing the effects of CaM or its mutant CaM_{1234} on the interaction between TRPP3 and CaMK2. Right panel: data from three independent experiments were quantified, normalized, and averaged. $^{***}p < 0.001$, ns: not significant.

of CaM on the channel (Fig. 6F), indicating that the inhibition of TRPP3 can be through phosphorylation of T591 or through disrupting the TRPP3/CaM binding. These data together demonstrated that CaM inhibits the TRPP3 channel function through recruiting its downstream kinase CaMK2 for phosphorylation of site T591 in the channel.

3. Discussion

We and other groups previously reported that human TRPP3 is regulated by a number of factors including Ca^{2+}, voltage, pH, amiloride analogs, large monovalent organic cations, troponin I, α-actinin and receptor for activated protein kinase 1 (RACK1) (Dai et al., 2006, 2007; DeCaen et al., 2016; Li et al., 2003, 2007; Liu et al., 2002; Yang et al., 2012). Extracellular Ca^{2+} has been shown to activate TRPP3, which is followed by channel inactivation/desensitization. One hypothetical mechanism is that accumulation of intracellular Ca^{2+} due to TRPP3-mediated Ca^{2+} entry enhances Ca^{2+} outward moving thereby blocking the conducting pore through interacting with residue D523 in the selectivity filter, resulting in channel inactivation (DeCaen et al., 2016). Interestingly, we previously showed that mutant D523N exhibits no Ca^{2+}-induced activation (Hussein et al., 2015), indicating that D523 is essential for channel activation. Further studies would be desired to confirm that D523 is involved in both the channel activation and the ensuing inactivation. As a Ca^{2+}-binding protein, CaM would affect intracellular accumulation of free Ca^{2+} and thus may affect TRPP3 channel inactivation based on the reported model (Hussein et al., 2015). Our current study showed that Ca^{2+}-induced TRPP3 activation is inhibited by Ca^{2+}/CaM through TRPP3 phosphorylation at T591 by CaMK2.

CaM is known to regulate membrane receptors (Zhang et al., 1998), transporters (Iwamoto et al., 2010) and a variety of ion channels including voltage-gated Ca^{2+} (DeMaria et al., 2001), Na^{+} (Ben-Johny

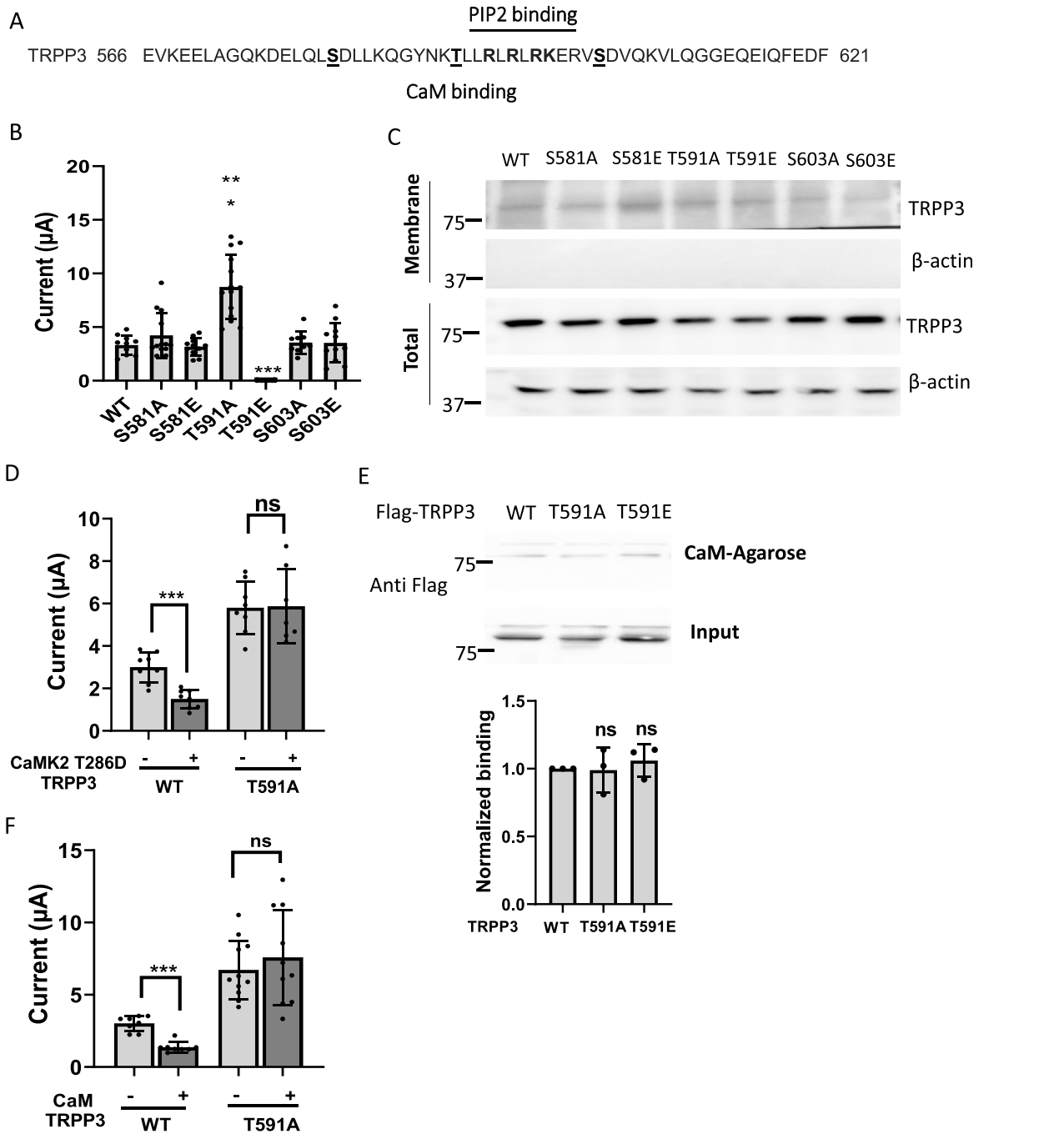

Fig. 6. Role of T591 in the TRPP3 channel function. A. CaM-binding domain identified in the TRPP3 C-terminus in which a PIP2-binding site and three potential phosphorylation residues (S or T) are indicated (bold and underlined). **B.** Averaged Ca^{2+}-activated currents (at −50 mV) of WT TRPP3 and indicated mutants expressed in three batches of oocytes. ***$p < 0.001$. **C.** Surface and total expression of WT TRPP3 and mutants in oocytes determined by biotinylation, with β-actin as a loading control, representative of three independent experiments. Alanine and aspartate substitutions mimic dephosphorylation and phosphorylation, respectively. **D.** Effects of CaMK2 T286D on the function of WT TRPP3 and the T591A mutant assessed by Ca^{2+}-activated currents (at −50 mV) averaged from three batches of oocytes. ***$p < 0.001$; ns: not significant. **E.** Effects of mutations at site 591 on the TRPP3/CaM binding determined by CaM-Agarose Pull-down. Upper panel: representative data showing the effects of the T591A and T591E mutations. Lower panel: data from three independent experiments were quantified, normalized, and averaged. ns: not significant. **F.** Effects of CaM on the function of WT TRPP3 and mutant T591A assessed by Ca^{2+}-activated currents (at −50 mV) averaged from three batches of oocytes. ***$p < 0.001$; ns: not significant.

et al., 2015) and K^+ channels (Schumacher et al., 2001) and TRP channels (Hasan & Zhang, 2018). Compared to other membrane proteins, how TRP channels are regulated by CaM is less understood, possibly because they are stimulated by diverse stimuli such as temperature, natural chemicals and mechanical force (Falcón et al., 2019). Several residues in TRPs have been reported to be involved in CaM binding by means of functional studies and *in vitro* or *in vivo* binding assays (Gordon-Shaag et al., 2008) but overall whether the regulation by CaM is through direct TRP/CaM binding or through an intermediate factor has yet to be determined by further studies. In fact, indirect CaM modulation mechanisms through altering channel/lipid interaction (Wang et al., 2001), channel biosynthesis (Deutsch, 2003), or membrane trafficking (Joiner et al., 2001) have been reported.

The highly Ca^{2+}-selective TRPV5 and TRPV6 possess CaMBDs in the

N- and C-termini as well as in transmembrane domains but some of these bindings remain debatable (Derler et al., 2006). Binding of CaM to one of these CaMBDs is known to act as a rapid feedback mechanism to prevent Ca^{2+} overload and maintain Ca^{2+} homeostasis (Kovalevskaya et al., 2012). In a proposed "two-tail" CaM modulation model, the CaM C-lobe constitutively binds to TRPV6 while the N-lobe promotes TRPV6 inactivation through Ca^{2+}-dependent conformational changes (Bate et al., 2018). However, this model was strongly challenged by recently resolved structures of the TRPV6/CaM and TRPV5/CaM complexes, which revealed that the CaM C-lobe plugs the channel through a unique cation-π interaction by inserting its K115 side chain to the TRPV6 pore's intracellular entrance thereby blocking pore conduction (Hughes et al., 2018; Singh et al., 2018). In contrast, the mechanism of inhibition of TRPC4 by CaM was different because the structures of the TRPC4 apo and TRPC4/CaM complex revealed their similar conducting pore conformations (Vinayagam et al., 2020). In fact, CaM binding resulted in a more stabilized closed state in which the channel periphery displays pronounced differences compared to that of TRPC4 apo. However, due to the lack of a fully resolved CaM structure in the TRPC4/CaM complex, it remains to be determined how CaM affects the overall conformation of TRPC4.

While Ca^{2+}-dependent CaM binding to these other TRP channels regulates their function through inducing channel conformational changes, our present study showed that CaM binding to TRPP3 inhibits its function through promoting phosphorylation of TRPP3 by CaMK2. Binding of CaM to a channel protein may allow an efficient and rapid response of the channel to Ca^{2+}, especially when the protein does not bind Ca^{2+} directly. However, of note, weak TRPP3/CaM binding was still detected in the absence of Ca^{2+} (Fig. 2D) or when Ca^{2+}-binding sites in TRPP3 were removed (Fig. 3C). This partial Ca^{2+} independence was similarly observed for L-type Ca^{2+} channel and TRPV1 (Numazaki et al., 2003; Peterson et al., 1999). We found that the TRPP3/CaM binding is necessary but not sufficient for channel inhibition. For example, the function of the TRPP3 mutant T591A became irresponsive to CaM while retaining its CaM binding ability (Fig. 6 E and F), which is consistent with our finding that TRPP3/CaM binding facilitates TRPP3 phosphorylation at T591 by kinase CaMK2, a mechanism similar to one proposed for a Na^{+} channel (Deschênes et al., 2002).

Regulation of TRPP3 by CaM has in fact also been explored by another group of researchers who proposed that the CaM N-lobe is involved in TRPP3 inhibition, with L593 acting as a CaM-binding residue (Baik et al., 2020). This infers that the channel activity of mutant L593A should be higher than that of WT TRPP3 due to the lack of inhibition by endogenous CaM in oocytes, which however, was not supported by our data (Fig. S1A). We also found that the L593A mutation does not affect the TRPP3/CaM interaction assessed by means of CaM agarose Pull-down assays (Fig. S1B), indicating that L593 is not involved in CaM binding. CaM is known to bind to an IQ motif or a hydrophobic alpha helix (Rhoads & Friedberg, 1997) but with exceptions (Mercado et al., 2010). Given the absence of an IQ motif in TRPP3, further studies would be needed to identify its CaM-binding residues. The EF-hand motif was shown to be important for gating of large conductance, Ca^{2+}-sensitive K^{+} and voltage-gated Na^{+} channels through Ca^{2+}-dependent conformational changes and intramolecular interaction with the III-IV intracellular linker, respectively (Braun & Sy, 2001; Gardill et al., 2018). However, in TRPP2, a TRPP3 homologue with 70% overall sequence similarity, the importance of the Ca^{2+}/EF-hand binding was controversial. One study showed that Ca^{2+} binding to the EF-hand is required for the TRPP2 channel function (Petri et al., 2010) while another study found that the Ca^{2+}/EF-hand binding is irrelevant to the channel function nor to the cystogenesis (Vien et al., 2020). The EF-hand in TRPP3 was reported to have no functional relevance importance(DeCaen et al., 2016; Li et al., 2002), which is consistent with our current finding that EF-hand deletion does not affect the inhibitory effect of CaM or the TRPP3/CaM interaction (Fig. 3 F and G).

Although we found competition between CaM and PIP2 for binding with TRPP3, unlike PIP2, CaM did not affect the TRPP3 N/C interaction (Fig. 4). In fact, several reports have found complex interplays between CaM and PIP2 (Alberdi et al., 2015; Cao et al., 2013; Tobelaim et al., 2017). While they exert similar inhibitory effects on the TRPP3 function, we don't know yet whether their binding sites (I560–F621 for CaM and R594Q/R596Q/R598Q/K599Q for PIP2) (22) have overlapping residues. Although CaM and PIP2 bind to overlapping regions in TRPV1 and TRPC6, they were found to bind with distinct residues and exhibited opposite functional effects (Kwon et al., 2007; Nilius et al., 2008). CaM and PIP2 demonstrated similar gating modulations on other channels such as Kv7.1 by stabilizing the open state (Trudeau & Zagotta, 2003). The fact that CaM and PIP2 have distinct ways by which they inhibit TRPP3 might be for different biological roles, for example, in response to distinct upstream signals. Interestingly, although it is well known that TRPP3 is activated by Ca^{2+} entry, which is followed by inactivation, the mechanisms underlying the activation and the ensuing inactivation are not well understood. We think that a phospholipase C (PLC)/PIP2 pathway may underly the Ca^{2+}-induced TRPP3 channel activation while the CaM/CaMKII pathway discovered in this study may account, at least in part, for the ensuing inactivation: at the basal state of TRPP3, the intracellular Ca^{2+} increase due to TRPP3-mediated Ca^{2+} entry activates PLC, which results in the hydrolysis of PIP2 thereby activating the channel and causing entry of more Ca^{2+} (and other cations as well), which then in turn activates the CaM/CaMKII pathway thereby inactivating TRPP3. This Ca^{2+} entry-induced sequential activation and inactivation through two distinct pathways may be important for preventing cells from Ca^{2+} overload.

Despite of high sequence homology between TRPP3 and TRPP2 and the presence of TRPP2/CaM interaction (Fig. S2A), we found that the TRPP2 function is insensitive to CaM (Fig. S2B). Interestingly, sequence alignment found that TRPP3 T591 corresponds to TRPP2 A711 (Fig. S2C), suggesting that TRPP2 may constitutively in its 'dephosphorylated' state at site 711. Indeed, constitutive mimic of phosphorylation by changing A711 to E or D in TRPP2 completely abolished the channel function (Fig. S2D).

In summary, we have identified that CaM binds to TRPP3 in competition with PIP2 and inhibits the TRPP3 channel function through a Ca2+/CaM/CaMKII pathway, which is distinct from how PIP2 inhibits TRPP3. Ca^{2+} entry through TRPP3 increases the formation of the CaM/Ca^{2+} complex that binds to the TRPP3 C-terminus, which enhances the TRPP3/CaMK2 interaction thereby promoting the T591 phosphorylation, which inhibits the channel function.

4. Methods

4.1. Plasmids, mutants, antibodies, and chemical reagents

Human Flag-TRPP3 cDNA was subcloned into *Xenopus* oocytes expression vector pCHGF (Yang et al., 2012). PEGFP-CaM WT and mutant plasmids were obtained from Dr. Veit Flocerzi's lab and subcloned into PGEMHE for oocytes expression. WT CaMK2 and mutant plasmids were kindly provided by Dr. Khaled Machaca (Weill Cornell Medicine, NY). Q5 master mix (NEB) was used to generate all the mutations, which were verified by sequencing. Antibodies against β-actin, GST, His, HA and Flag were purchased from Santa Cruz Biotechnology (Santa Cruz, CA). The antibody against CaM was purchased from Cell Signaling Technology (Whitby, Ontario). The antibody against CaMK2 was purchased from Abcam (Cambridge, UK). Secondary antibodies were purchased from GE Healthcare (Waukesha, WI). NFA, CMZ, KN93 and AIP were purchased from Millipore Sigma Canada (Oakville, ON) and diC_8-PIP2 was from Echelon Biosciences (Salt Lake City, UT).

4.2. Xenopus oocyte expression

Capped RNAs encoding TRPP3, CaM and CaMK2 were synthesized by an *in vitro* transcription T7 mMESSAGE mMACHINE kit (Ambion, Austin,

TX) and injected (25–50 ng per oocyte) into *Xenopus* oocytes prepared as described (Cai et al., 2020). Same amount of water was injected to the oocytes served as control. Oocytes were incubated at 18°C for 2–3 days before electrophysiological measurements. The present study was under the approvement of the Ethical Committee for Animal Experiments of the University of Alberta and performed in accordance with the Guidelines for Research with Experimental Animals of the University of Alberta and the Guide for the Care and Use of Laboratory Animals (NIH Guide) revised in 1996.

4.3. Two-electrode voltage clamp electrophysiology

The two-electrode voltage clamp electrophysiology experiments in *Xenopus* oocytes were performed as we described previously (Zheng et al., 2018). Briefly, the electrodes (Capillary pipettes, Warner Instruments, Hamden, CT) that impale an oocyte were filled with 3 M KCl to form a tip resistance of 0.3–2 MΩ. Duration of application of extracellular Ca^{2+}, CMZ was indicated in time course recordings. Unless described otherwise, measurements were performed when an oocyte was voltage clamped and held at −50 mV. Whole-cell currents and membrane potentials were recorded and analyzed using a Geneclamp 500B amplifier and Digidata 1322A AD/DA converter (Molecular Devices, Union City, CA) together with the pClamp 9 software (Axon Instruments, Union City, CA). Current and voltage signals were digitized at 100 μs/sample and filtered at 2 kHz through a Bessel filter. SigmaPlot 13 (Systat Software, San Jose, CA) and GraphPad Prism 8 (GraphPad Software, San Diego, CA) were used for data plotting.

4.4. Surface protein biotinylation

Xenopus oocytes after three times washing with ice-cold PBS solution were incubated with 0.5 mg/ml sulfo-NHS-SS-Biotin (Pierce, Rockford, IL) for 30 min at room temperature. Non-reacted biotin was quenched by 1 M NH_4Cl. Oocytes were then washed with ice-cold PBS solution and harvested in ice-cold CelLytic M lysis buffer (Sigma) supplemented with proteinase inhibitor cocktail (Thermo Scientific, Waltham, MA). Upon addition of 100 μl streptavidin (Pierce), lysates were incubated at 4°C overnight with gentle shaking. The surface protein bound to streptavidin was resuspended in SDS loading buffer and subjected to SDS-PAGE.

4.5. Co-IP, CaM-Agarose Pull-down and GST Pull-down

Co-IP experiments were performed as we previously described (Zheng et al., 2018). Briefly, a group of 20–30 oocytes washed with PBS were solubilized in ice-cold CelLytic-M lysis buffer (Sigma) supplemented with proteinase inhibitor cocktail. Supernatants were collected after centrifugation at 13,200 rpm for 15 min and precleaned for 1 h with 50% protein G-Sepharose (GE Healthcare), followed by incubation with indicated antibodies at 4°C for 4 h. Upon the addition of 100 μl of 50% protein G-Sepharose, the mixture was incubated at 4°C overnight with gentle shaking. The immune complexes conjugated to protein G-Sepharose were washed three times with cold PBS solution containing 1% Nonidet P-40 and eluted by SDS loading buffer. Precipitated proteins were subjected to western blot analysis.

Cell lysates were prepared same as above. 100 μL CaM-Agarose beads (Sigma) were added to the supernatants and the mixture was incubated at 4°C overnight with gentle shaking. Unless indicated, 1 mM Ca^{2+} was included in the mixture to increase the affinity. The beads were then washed three times with cold PBS solution containing 1% Nonidet P-40 and eluted by SDS loading buffer. Precipitated proteins were subjected to western blot analysis.

GST- or His-tagged human TRPP3 peptides or CaM were purified from *E. coli* and solubilized in the CelLytic-M lysis buffer (Sigma) and incubated at the same amount (2 μg) at 4°C for 4 h with gentle shaking, followed by overnight incubation after addition of 50 μL Glutathione Sepharose 4B agarose beads (GE Healthcare). The beads were then washed three times with PBS buffer with 1% Nonidet P-40, and the remaining proteins were eluted using SDS loading buffer and were subjected to western blot analysis.

5. Statistical analysis

All statistical data in this study are represented as mean ± SD (standard deviation) from N measurements. Student's t-tests were used to compare two groups of data; One-way ANOVA was used to compare multiple groups. *, ** and *** indicate $p < 0.05$, 0.01 and 0.001, respectively; ns indicates statistically not significant.

Author contributions

Conceptualization, X.L. and X.-Z.C.; Investigation, X.L., Y.W., Z.W., Q.X. and C.Z.; Supervision, J.T. and X.-Z.C. Writing, X.L. and X.-Z.C.

Disclosure

Competing financial interests: The Authors declare no competing financial interest.

Acknowledgments

This work was supported by the Natural Sciences and Engineering Research Council of Canada (to X.Z.C.), Kidney Foundation of Canada (to X.Z.C.) and National Natural Science Foundation of China (grant # 31871176 and 32070726, to J.T.). X.L. was a recipient of the Alberta Graduate Excellence Scholarship (AGES).

Appendix A. Supplementary data

Supplementary data to this article can be found online at https://doi.org/10.1016/j.cellin.2023.100088.

References

Alberdi, A., Gomis-Perez, C., Bernardo-Seisdedos, G., Alaimo, A., Malo, C., Aldaregia, J., Lopez-Robles, C., Areso, P., Butz, E., Wahl-Schott, C., et al. (2015). Uncoupling PIP2-calmodulin regulation of Kv7.2 channels by an assembly destabilizing epileptogenic mutation. *Journal of Cell Science, 128*, 4014–4023.

Baik, J. Y., Park, E. Y. J., & So, I. (2020). Ca(2+)/calmodulin-dependent regulation of polycystic kidney disease 2-like-1 by binding at C-terminal domain. *Korean Journal Of Physiology And Pharmacology, 24*, 277–286.

Bate, N., Caves, R. E., Skinner, S. P., Goult, B. T., Basran, J., Mitcheson, J. S., & Vuister, G. W. (2018). A novel mechanism for calmodulin-dependent inactivation of transient receptor potential vanilloid 6. *Biochemistry, 57*, 2611–2622.

Ben Johny, M., Yang, P. S., Bazzazi, H., & Yue, D. T. (2013). Dynamic switching of calmodulin interactions underlies Ca2+ regulation of CaV1.3 channels. *Nature Communications, 4*, 1717.

Ben-Johny, M., Dick, I. E., Sang, L., Limpitikul, W. B., Kang, P. W., Niu, J., Banerjee, R., Yang, W., Babich, J. S., Issa, J. B., et al. (2015). Towards a unified theory of calmodulin regulation (calmodulation) of voltage-gated calcium and sodium channels. *Current Molecular Pharmacology, 8*, 188–205.

Braun, A. P., & Sy, L. (2001). Contribution of potential EF hand motifs to the calcium-dependent gating of a mouse brain large conductance, calcium-sensitive K(+) channel. *Journal of Physiology, 533*, 681–695.

Cai, R., Liu, X., Zhang, R., Hofmann, L., Zheng, W., Amin, M. R., Wang, L., Hu, Q., Peng, J. B., Michalak, M., et al. (2020). Autoinhibition of TRPV6 channel and regulation by PIP2. *iScience, 23*, Article 101444.

Cao, C., Zakharian, E., Borbiro, I., & Rohacs, T. (2013). Interplay between calmodulin and phosphatidylinositol 4,5-bisphosphate in Ca2+-induced inactivation of transient receptor potential vanilloid 6 channels. *Journal of Biological Chemistry, 288*, 5278–5290.

Chin, D., & Means, A. R. (2000). Calmodulin: A prototypical calcium sensor. *Trends in Cell Biology, 10*, 322–328.

Dai, X. Q., Karpinski, E., & Chen, X. Z. (2006). Permeation and inhibition of polycystin-L channel by monovalent organic cations. *Biochimica et Biophysica Acta, 1758*, 197–205.

Dai, X. Q., Ramji, A., Liu, Y., Li, Q., Karpinski, E., & Chen, X. Z. (2007). Inhibition of TRPP3 channel by amiloride and analogs. *Molecular Pharmacology, 72*, 1576–1585.

DeCaen, P. G., Delling, M., Vien, T. N., & Clapham, D. E. (2013). Direct recording and molecular identification of the calcium channel of primary cilia. *Nature, 504*, 315–318.

DeCaen, P. G., Liu, X., Abiria, S., & Clapham, D. E. (2016). Atypical calcium regulation of the PKD2-L1 polycystin ion channel. *Elife, 5*.
Delling, M., DeCaen, P. G., Doerner, J. F., Febvay, S., & Clapham, D. E. (2013). Primary cilia are specialized calcium signalling organelles. *Nature, 504*, 311–314.
DeMaria, C. D., Soong, T. W., Alseikhan, B. A., Alvania, R. S., & Yue, D. T. (2001). Calmodulin bifurcates the local Ca2+ signal that modulates P/Q-type Ca2+ channels. *Nature, 411*, 484–489.
Derler, I., Hofbauer, M., Kahr, H., Fritsch, R., Muik, M., Kepplinger, K., Hack, M. E., Moritz, S., Schindl, R., Groschner, K., et al. (2006). Dynamic but not constitutive association of calmodulin with rat TRPV6 channels enables fine tuning of Ca2+-dependent inactivation. *Journal of Physiology, 577*, 31–44.
Deschênes, I., Neyroud, N., DiSilvestre, D., Marbán, E., Yue, D. T., & Tomaselli, G. F. (2002). Isoform-specific modulation of voltage-gated Na(+) channels by calmodulin. *Circulation Research, 90*, E49–E57.
Deutsch, C. (2003). The birth of a channel. *Neuron, 40*, 265–276.
Dosemeci, A., & Jaffe, H. (2010). Regulation of phosphorylation at the postsynaptic density during different activity states of Ca2+/calmodulin-dependent protein kinase II. *Biochemical and Biophysical Research Communications, 391*, 78–84.
Falcón, D., Galeano-Otero, I., Calderón-Sánchez, E., Del, T. R., Martín-Bórnez, M., Rosado, J. A., Hmadcha, A., & Smani, T. (2019). TRP channels: Current perspectives in the adverse cardiac remodeling. *Frontiers in Physiology, 10*, 159.
Gabelli, S. B., Yoder, J. B., Tomaselli, G. F., & Amzel, L. M. (2016). Calmodulin and Ca(2+) control of voltage gated Na(+) channels. *Channels, 10*, 45–54.
Gardill, B. R., Rivera-Acevedo, R. E., Tung, C. C., Okon, M., McIntosh, L. P., & Van, P. F. (2018). The voltage-gated sodium channel EF-hands form an interaction with the III-IV linker that is disturbed by disease-causing mutations. *Scientific Reports, 8*, 4483.
Gordon-Shaag, A., Zagotta, W. N., & Gordon, S. E. (2008). Mechanism of Ca(2+)-dependent desensitization in TRP channels. *Channels, 2*, 125–129.
Hasan, R., & Zhang, X. (2018). Ca(2+) regulation of TRP ion channels. *International Journal of Molecular Sciences, 19*.
Huang, R. Y., Laing, J. G., Kanter, E. M., Berthoud, V. M., Bao, M., Rohrs, H. W., Townsend, R. R., & Yamada, K. A. (2011). Identification of CaMKII phosphorylation sites in Connexin43 by high-resolution mass spectrometry. *Journal of Proteome Research, 10*, 1098–1109.
Hughes, T. E. T., Pumroy, R. A., Yazici, A. T., Kasimova, M. A., Fluck, E. C., Huynh, K. W., Samanta, A., Molugu, S. K., Zhou, Z. H., Carnevale, V., et al. (2018). Structural insights on TRPV5 gating by endogenous modulators. *Nature Communications, 9*, 4198.
Hussein, S., Zheng, W., Dyte, C., Wang, Q., Yang, J., Zhang, F., Tang, J., Cao, Y., & Chen, X. Z. (2015). Acid-induced off-response of PKD2L1 channel in Xenopus oocytes and its regulation by Ca(2.). *Scientific Reports, 5*, Article 15752.
Ishimaru, Y., Inada, H., Kubota, M., Zhuang, H., Tominaga, M., & Matsunami, H. (2006). Transient receptor potential family members PKD1L3 and PKD2L1 form a candidate sour taste receptor. *Proceedings of the National Academy of Sciences of the U S A, 103*, 12569–12574.
Iwamoto, N., Lu, R., Tanaka, N., be-Dohmae, S., & Yokoyama, S. (2010). Calmodulin interacts with ATP binding cassette transporter A1 to protect from calpain-mediated degradation and upregulates high-density lipoprotein generation. *Arteriosclerosis, Thrombosis, and Vascular Biology, 30*, 1446–1452.
Joiner, W. J., Khanna, R., Schlichter, L. C., & Kaczmarek, L. K. (2001). Calmodulin regulates assembly and trafficking of SK4/Ik1 Ca2+-activated K+ channels. *Journal of Biological Chemistry, 276*, 37980–37985.
Kovalevskaya, N. V., Bokhovchuk, F. M., & Vuister, G. W. (2012). The TRPV5/6 calcium channels contain multiple calmodulin binding sites with differential binding properties. *Journal of Structural and Functional Genomics, 13*, 91–100.
Kwon, Y., Hofmann, T., & Montell, C. (2007). Integration of phosphoinositide- and calmodulin-mediated regulation of TRPC6. *Molecular Cell, 25*, 491–503.
Li, Q., Dai, X. Q., Shen, P. Y., Wu, Y., Long, W., Chen, C. X., Hussain, Z., Wang, S., & Chen, X. Z. (2007). Direct binding of alpha-actinin enhances TRPP3 channel activity. *Journal of Neurochemistry, 103*, 2391–2400.
Li, Q., Liu, Y., Shen, P. Y., Dai, X. Q., Wang, S., Smillie, L. B., Sandford, R., & Chen, X. Z. (2003). Troponin I binds polycystin-L and inhibits its calcium-induced channel activation. *Biochemistry, 42*, 7618–7625.
Li, Q., Liu, Y., Zhao, W., & Chen, X. Z. (2002). The calcium-binding EF-hand in polycystin-L is not a domain for channel activation and ensuing inactivation. *FEBS Letters, 516*, 270–278.
Liu, Y., Li, Q., Tan, M., Zhang, Y. Y., Karpinski, E., Zhou, J., & Chen, X. Z. (2002). Modulation of the human polycystin-L channel by voltage and divalent cations. *FEBS Letters, 525*, 71–76.
Lu, Z., Cui, Y., Wei, X., Gao, P., Zhang, H., Wei, X., Li, Q., Sun, F., Yan, Z., Zheng, H., et al. (2018). Deficiency of PKD2L1 (TRPP3) exacerbates pathological cardiac hypertrophy by augmenting NCX1-mediated mitochondrial calcium overload. *Cell Reports, 24*, 1639–1652.
Mercado, J., Gordon-Shaag, A., Zagotta, W. N., & Gordon, S. E. (2010). Ca2+-dependent desensitization of TRPV2 channels is mediated by hydrolysis of phosphatidylinositol 4,5-bisphosphate. *Journal of Neuroscience, 30*, 13338–13347.
Nilius, B., Owsianik, G., & Voets, T. (2008). Transient receptor potential channels meet phosphoinositides. *EMBO Journal, 27*, 2809–2816.
Nomura, H., Turco, A. E., Pei, Y., Kalaydjieva, L., Schiavello, T., Weremowicz, S., Ji, W., Morton, C. C., Meisler, M., Reeders, S. T., et al. (1998). Identification of PKDL, a novel polycystic kidney disease 2-like gene whose murine homologue is deleted in mice with kidney and retinal defects. *Journal of Biological Chemistry, 273*, 25967–25973.
Numazaki, M., Tominaga, T., Takeuchi, K., Murayama, N., Toyooka, H., & Tominaga, M. (2003). Structural determinant of TRPV1 desensitization interacts with calmodulin. *Proceedings of the National Academy of Sciences of the U S A, 100*, 8002–8006.
Park, E. Y. J., Baik, J. Y., Kwak, M., & So, I. (2019). The role of calmodulin in regulating calcium-permeable PKD2L1 channel activity. *KOREAN JOURNAL OF PHYSIOLOGY and PHARMACOLOGY, 23*, 219–227.
Park, E. Y. J., Kwak, M., Ha, K., & So, I. (2018). Identification of clustered phosphorylation sites in PKD2L1: How PKD2L1 channel activation is regulated by cyclic adenosine monophosphate signaling pathway. *Pflügers Archiv, 470*, 505–516.
Pei, Y. (2003). Molecular genetics of autosomal dominant polycystic kidney disease. *Clinical and Investigative Medicine, 26*, 252–258.
Peterson, B. Z., DeMaria, C. D., Adelman, J. P., & Yue, D. T. (1999). Calmodulin is the Ca2+ sensor for Ca2+ -dependent inactivation of L-type calcium channels. *Neuron, 22*, 549–558.
Petri, E. T., Celic, A., Kennedy, S. D., Ehrlich, B. E., Boggon, T. J., & Hodsdon, M. E. (2010). Structure of the EF-hand domain of polycystin-2 suggests a mechanism for Ca2+-dependent regulation of polycystin-2 channel activity. *Proceedings of the National Academy of Sciences of the U S A, 107*, 9176–9181.
Rhoads, A. R., & Friedberg, F. (1997). Sequence motifs for calmodulin recognition. *The FASEB Journal, 11*, 331–340.
Schumacher, M. A., Rivard, A. F., Bächinger, H. P., & Adelman, J. P. (2001). Structure of the gating domain of a Ca2+-activated K+ channel complexed with Ca2+/calmodulin. *Nature, 410*, 1120–1124.
Singh, A. K., McGoldrick, L. L., Twomey, E. C., & Sobolevsky, A. I. (2018). Mechanism of calmodulin inactivation of the calcium-selective TRP channel TRPV6. *Science Advances, 4*, Article eaau6088.
Songyang, Z., Lu, K. P., Kwon, Y. T., Tsai, L. H., Filhol, O., Cochet, C., Brickey, D. A., Soderling, T. R., Bartleson, C., Graves, D. J., et al. (1996). A structural basis for substrate specificities of protein ser/thr kinases: Primary sequence preference of casein kinases I and II, NIMA, phosphorylase kinase, calmodulin-dependent kinase II, CDK5, and Erk1. *Molecular and Cellular Biology, 16*, 6486–6493.
Stefan, M. I., Edelstein, S. J., & Le, N. N. (2008). An allosteric model of calmodulin explains differential activation of PP2B and CaMKII. *Proceedings of the National Academy of Sciences of the U S A, 105*, 10768–10773.
Sternberg, J. R., Prendergast, A. E., Brosse, L., Cantaut-Belarif, Y., Thouvenin, O., Orts-Del'Immagine, A., Castillo, L., Djenoune, L., Kurisu, S., McDearmid, J. R., et al. (2018). Pkd2l1 is required for mechanoception in cerebrospinal fluid-contacting neurons and maintenance of spine curvature. *Nature Communications, 9*, 3804.
Sun, L., Hodeify, R., Haun, S., Charlesworth, A., MacNicol, A. M., Ponnappan, S., Ponnappan, U., Prigent, C., & Machaca, K. (2008). Ca2+ homeostasis regulates Xenopus oocyte maturation. *Biology of Reproduction, 78*, 726–735.
Tobelaim, W. S., Dvir, M., Lebel, G., Cui, M., Buki, T., Peretz, A., Marom, M., Haitin, Y., Logothetis, D. E., Hirsch, J. A., et al. (2017). Competition of calcified calmodulin N lobe and PIP2 to an LQT mutation site in Kv7.1 channel. *Proceedings of the National Academy of Sciences of the U S A, 114*, E869–E878.
Trudeau, M. C., & Zagotta, W. N. (2002). Mechanism of calcium/calmodulin inhibition of rod cyclic nucleotide-gated channels. *Proceedings of the National Academy of Sciences of the U S A, 99*, 8424–8429.
Trudeau, M. C., & Zagotta, W. N. (2003). Calcium/calmodulin modulation of olfactory and rod cyclic nucleotide-gated ion channels. *Journal of Biological Chemistry, 278*, 18705–18708.
Vangeel, L., & Voets, T. (2019). Transient receptor potential channels and calcium signaling. *Cold Spring Harbor Perspectives in Biology, 11*.
Vien, T. N., Ng, L. C. T., Smith, J. M., Dong, K., Krappitz, M., Gainullin, V. G., Fedeles, S., Harris, P. C., Somlo, S., & DeCaen, P. G. (2020). Disrupting polycystin-2 EF hand Ca(2+) affinity does not alter channel function or contribute to polycystic kidney disease. *Journal of Cell Science, 133*.
Vinayagam, D., Quentin, D., Yu-Strzelczyk, J., Sitsel, O., Merino, F., Stabrin, M., Hofnagel, O., Yu, M., Ledeboer, M. W., Nagel, G., et al. (2020). Structural basis of TRPC4 regulation by calmodulin and pharmacological agents. *Elife, 9*.
Wang, J., Arbuzova, A., Hangyás-Mihályné, G., & McLaughlin, S. (2001). The effector domain of myristoylated alanine-rich C kinase substrate binds strongly to phosphatidylinositol 4,5-bisphosphate. *Journal of Biological Chemistry, 276*, 5012–5019.
Wang, Z., Ng, C., Liu, X., Wang, Y., Li, B., Kashyap, P., Chaudhry, H. A., Castro, A., Kalontar, E. M., Ilyayev, L., et al. (2019). The ion channel function of polycystin-1 in the polycystin-1/polycystin-2 complex. *EMBO Reports, 20*, Article e48336.
Wen, H., & Levitan, I. B. (2002). Calmodulin is an auxiliary subunit of KCNQ2/3 potassium channels. *Journal of Neuroscience, 22*, 7991–8001.
White, R. R., Kwon, Y. G., Taing, M., Lawrence, D. S., & Edelman, A. M. (1998). Definition of optimal substrate recognition motifs of Ca2+-calmodulin-dependent protein kinases IV and II reveals shared and distinctive features. *Journal of Biological Chemistry, 273*, 3166–3172.
Wu, G., Hayashi, T., Park, J. H., Dixit, M., Reynolds, D. M., Li, L., Maeda, Y., Cai, Y., Coca-Prados, M., & Somlo, S. (1998). Identification of PKD2L, a human PKD2-related gene: Tissue-specific expression and mapping to chromosome 10q25. *Genomics, 54*, 564–568.
Yang, J., Wang, Q., Zheng, W., Tuli, J., Li, Q., Wu, Y., Hussein, S., Dai, X. Q., Shafiei, S., Li, X. G., et al. (2012). Receptor for activated C kinase 1 (RACK1) inhibits function of

transient receptor potential (TRP)-type channel Pkd2L1 through physical interaction. *Journal of Biological Chemistry, 287*, 6551–6561.

Zhang, S., Ehlers, M. D., Bernhardt, J. P., Su, C. T., & Huganir, R. L. (1998). Calmodulin mediates calcium-dependent inactivation of N-methyl-D-aspartate receptors. *Neuron, 21*, 443–453.

Zheng, W., Cai, R., Hofmann, L., Nesin, V., Hu, Q., Long, W., Fatehi, M., Liu, X., Hussein, S., Kong, T., et al. (2018). Direct binding between pre-S1 and TRP-like domains in TRPP channels mediates gating and functional regulation by PIP2. *Cell Reports, 22*, 1560–1573.

Zheng, W., Yang, J., Beauchamp, E., Cai, R., Hussein, S., Hofmann, L., Li, Q., Flockerzi, V., Berthiaume, L. G., Tang, J., et al. (2016). Regulation of TRPP3 channel function by N-terminal domain palmitoylation and phosphorylation. *Journal of Biological Chemistry, 291*, 25678–25691.